Gold–Boron Chemistry. Part 3.[1] The Synthesis, Characterisation, and Molecular Structure of $[(H_{11}C_6)_3PAu]_2B_8H_{10}$.† Comments on the 'Anomalous' Structure of B_8H_{12}

Andrew J. Wynd and Alan J. Welch *
Department of Chemistry, University of Edinburgh, Edinburgh EH9 3JJ

The reaction between $[AuMe\{P(C_6H_{11})_3\}]$ and $B_{10}H_{12}(PPh_3)_2$ yields an unexpected product, $[(H_{11}C_6)_3PAu]_2B_8H_{10}$ This complex was identified by multinuclear n.m.r. spectroscopy, and by a single-crystal *X*-ray diffraction study. Four molecules of $[(H_{11}C_6)_3PAu]_2B_8H_{10}$ and eight of water cocrystallise in space group *C*2/*c* with $a = 17.506(7)$, $b = 14.064(3)$, and $c = 20.179(3)$ Å, and $\beta = 105.012(22)°$; $R = 0.0469$ for 2 512 observed data. The gold–borane complex has crystallographically imposed C_2 molecular symmetry, the $\{Au_2B_8H_{10}\}$ fragment having effective C_{2v} symmetry. The complex is described as an eight-vertex borane cluster with two μ_3 gold phosphine units, and an analogy is drawn between the structure of $[(H_{11}C_6)_3PAu]_2B_8H_{10}$ and that of B_8H_{12}, a species whose structure is anomalous in terms of established electron-counting rules. Molecular orbital calculations show that, given the structures they have, the observed electron counts for $[(H_{11}C_6)_3PAu]_2B_8H_{10}$ and B_8H_{12} afford thermodynamically stable compounds.

Previous contributions to this series[1,2] have documented the syntheses and molecular and electronic structures of gold–borane complexes in which the gold atom acts as a μ or μ_4 bridge, and is not formally considered as a polyhedral vertex.

The gold–borane systems we have so far described are derived from *nido*-$B_{10}H_{14}$, and during their syntheses the integrity of the $\{B_{10}\}$ cluster is retained. We now report that reaction of $[AuMe\{P(C_6H_{11})_3\}]$ with *arachno*-$B_{10}H_{12}(PPh_3)_2$ causes partial degradation of the $\{B_{10}\}$ cluster, affording $[(H_{11}C_6)_3PAu]_2B_8H_{10}$. In this molecule the gold atoms are again non-vertex, but this time occupying μ_3 positions. Some aspects of this work have been previously communicated.[3]

Experimental

Details of the general experimental techniques and equipment used can be found in a previous contribution.[2] N.m.r. chemical shifts are reported relative to external $SiMe_4$ (^1H), 85% H_3PO_4 (^{31}P), and $BF_3{\cdot}OEt_2$ (^{11}B), with positive shifts to high frequency.

Syntheses.—The compound $[AuMe\{P(C_6H_{11})_3\}]$ was synthesised according to literature methods,[2] and its purity checked by ^{31}P-$\{^1H\}$ n.m.r. spectroscopy prior to use.

$B_{10}H_{12}(PPh_3)_2$. This product has been reported in the literature,[4] but no experimental details were given. Decaborane(14) (1.023 g, 8.373 mmol) and triphenylphosphine (4.413 g, 16.84 mmol) were stirred in ethoxyethane (20 cm^3) for 2 h at room temperature, during which time gaseous evolution was noted, along with deposition of a white solid. The precipitate was isolated by filtration, washed with ethoxyethane, and dried *in vacuo*. Yield 4.513 g, 83.7%. It may be recrystallised from dichloromethane–hexane in analytically pure form.

$[(H_{11}C_6)_3PAu]_2B_8H_{10}$. To a stirred mixture of $[AuMe\{P(C_6H_{11})_3\}]$ (0.1313 g, 0.267 mmol) and $B_{10}H_{12}(PPh_3)_2$ (0.1834 g, 0.285 mmol) was added dichloromethane (20 cm^3). Over a period of *ca.* 18 h the solution slowly became yellow. The solvent was removed *in vacuo* to yield a yellow-white powder. This was dissolved in the minimum amount of dichloromethane and chromatographed on an alumina column (6 × 2 cm) using tetrahydrofuran as stationary phase and eluant. The mobile yellow band was collected, and the solvent removed *in vacuo* to yield a yellow solid. Yellow crystals of $[(H_{11}C_6)_3PAu]_2B_8H_{10}{\cdot}2H_2O$ were grown from this by diffusion of hexane into a concentrated dichloromethane solution. Yield 21.4 mg, 15.3%. N.m.r. (CD_2Cl_2): ^{11}B-$\{^1H\}$, δ 1.49 (4B), −27.56 (2B), and −21.86 (2B); ^1H-$\{^{11}B\}$, δ 4.44, 0.65, and 0.18 (all BH); −2.90 (B–H–B); ^{31}P-$\{^1H\}$, δ 68.93 p.p.m.

Crystallographic Studies.—Graphite-monochromated Mo-K_α *X*-radiation, $\lambda = 0.710\,69$ Å, ω—2θ scans in 96 steps with ω scan width $= 0.8 + 0.35 \tan\theta$.

Crystal data. $C_{36}H_{76}Au_2B_8P_2{\cdot}2H_2O$, $M = 1\,087.4$, monoclinic, space group *C*2/*c*, $a = 17.506(7)$, $b = 14.064(3)$, $c = 20.179(3)$ Å, $\beta = 105.012(22)°$, $U = 4\,798.5$ Å^3, $Z = 4$, $D_c = 1\,505$ g cm^{-3}, μ(Mo-K_α) = 6.17 mm^{-1}, $F(000) = 2\,160$.

Data collection and processing. 2 936 Unique data were measured of which 2 512 with $F > 1\sigma(F)$ were retained; $\theta_{max.} = 22°$, $+h + k \pm l$. Crystal decayed by *ca.* 10% over the data collection period, for which correction was applied. The data were further corrected for Lorentz and polarisation effects (CADABS),[5] and then weighted according to $w^{-1} = [\sigma^2(F) + 0.002\,726(F)^2]$. After isotropic convergence, data were empirically corrected for absorption effects (DIFABS).[6]

Structure solution and refinement. The gold position was determined by automatic direct methods (SHELX 86),[7] all others by subsequent iterative ΔF syntheses and least-squares refinement (SHELX 76).[8] The cocrystallisation of one molecule of water (the origin of which is assumed to be imperfectly dried dichloromethane) per asymmetric unit was unexpected. Cage and solvate hydrogen atoms could not be satisfactorily located and remain absent. Organic hydrogen atoms were set in calculated positions (C–H 1.08 Å), riding on their respective C atom. Gold, phosphorus, boron, carbon, and oxygen atoms were allowed anisotropic thermal motion. A group thermal parameter for cyclohexyl H atoms was refined, converging at 0.162(11) Å^2. $R = 0.0469$, $R' = 0.0679$, $S = 1.109$. Data: variable ratio = 11:1, and maximum and minimum residues in

† *Supplementary data available:* see Instructions for Authors, *J. Chem. Soc., Dalton Trans.*, 1990, Issue 1, pp. xix—xxii.

Non-S.I. unit employed: eV ≈ 1.60 × 10^{-19} J.

Table 1. Fractional co-ordinates of non-hydrogen atoms in $[(H_{11}C_6)_3PAu]_2B_8H_{10}$

Atom	*x*	*y*	*z*
Au(6)	0.562 68(3)	0.024 23(3)	0.673 46(2)
P	0.616 15(16)	−0.114 39(21)	0.643 94(14)
B(1)	0.542 9(8)	0.219 5(8)	0.781 1(7)
B(2)	0.542 4(8)	0.174 5(9)	0.699 0(6)
B(5)	0.605 5(7)	0.122 0(10)	0.776 4(7)
B(7)	0.444 9(7)	0.122 5(9)	0.661 9(6)
C(11)	0.542 9(7)	−0.201 5(8)	0.596 1(6)
C(12)	0.575 2(7)	−0.296 6(7)	0.583 1(6)
C(13)	0.511 1(9)	−0.367 1(11)	0.548 5(8)
C(14)	0.459 2(11)	−0.325 6(11)	0.487 3(8)
C(15)	0.422 3(7)	−0.230 4(10)	0.499 5(7)
C(16)	0.488 0(8)	−0.163 2(10)	0.532 9(7)
C(21)	0.685 2(8)	−0.091 9(9)	0.591 2(6)
C(22)	0.750 0(7)	−0.159 8(9)	0.594 1(7)
C(23)	0.800 7(10)	−0.134 9(12)	0.544 8(10)
C(24)	0.816 1(12)	−0.039 4(14)	0.538 8(13)
C(25)	0.751 3(15)	0.027 6(12)	0.530 3(11)
C(26)	0.699 1(13)	0.005 0(11)	0.579 1(13)
C(31)	0.670 4(7)	−0.177 3(9)	0.720 5(5)
C(32)	0.611 6(8)	−0.215 8(10)	0.760 0(6)
C(33)	0.661 8(11)	−0.270 3(14)	0.826 4(8)
C(34)	0.717 8(11)	−0.198 1(18)	0.874 2(8)
C(35)	0.773 2(8)	−0.158 8(15)	0.833 7(7)
C(36)	0.731 7(8)	−0.112 2(11)	0.767 9(6)
O	0.426 2(13)	0.480 7(10)	0.263 5(14)

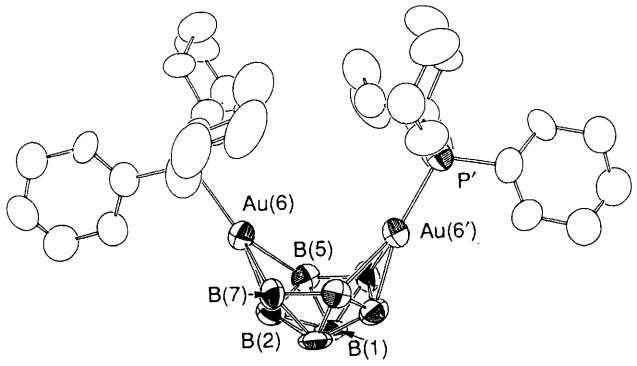

Figure 1. Perspective view of $[(H_{11}C_6)_3PAu]_2B_8H_{10}$ (**1**), with thermal ellipsoids drawn at the 50% probability level

final ΔF map 0.12 and −0.08 e Å^{-3} respectively. Atomic co-ordinates of refined atoms are given in Table 1. Scattering factors for carbon, hydrogen, oxygen, phosphorus, and boron were those inlaid in SHELX 76, whilst those for gold were taken from ref. 9. Molecular geometry calculations were performed by CALC,[10] and diagrams produced by EASYORTEP,[11] a modified version of ORTEP II.[12]

Additional material available from the Cambridge Crystallographic Data Centre comprises H-atom co-ordinates, thermal parameters, and remaining bond lengths and angles.

Molecular Orbital Calculation.—An extended-Hückel molecular orbital (EHMO) calculation was performed on an idealised model of $\{B_8H_{10}\}^{2-}$. The model was derived from the crystallographically determined structure of *arachno*-$[B_{10}H_{14}]^{2-}$ from which the $\{B(6)H_2\}$ and $\{B(9)H_2\}$ [numbering as in Figure 2(*b*)] fragments were removed. Co-ordinates of the remaining atoms were adjusted to give the model full C_{2v} symmetry. The calculation was performed using a locally modified version of ICON 8[13] and the weighted H_{ij} formula.[14] Full charge iteration at the highest possible level (including Madelung correction) was employed. The Slater exponent for H(1*s*), B(2*s*), and B(2*p*) was 1.30.

Results and Discussion

The room-temperature reaction between equivalent amounts of $[AuMe\{P(C_6H_{11})_3\}]$ and *arachno*-$B_{10}H_{12}(PPh_3)_2$ in dichloromethane yields $[(H_{11}C_6)_3PAu]_2B_8H_{10}$ (**1**) as the only isolable product. After work-up involving column chromatography and crystallisation the yield is *ca.* 30% of the theoretical maximum.

The ^{11}B-$\{^1H\}$ n.m.r. spectrum of (**1**) consists of three peaks of relative integrals 4:2:2, consistent with C_{2v} symmetry, although the broadness of the highest-frequency resonance might imply that this relatively high symmetry is beginning to break down (see later). The ^{11}B n.m.r. spectrum clearly shows that each boron atom is associated with an *exo*-terminal H atom, and ^1H-$\{^{11}B$, selective$\}$ n.m.r. spectroscopy reveals that those boron atoms whose resonance is of relative integral 4 additionally couple to the (two) bridging H atoms.

These spectroscopic data are consistent with the molecular structure of (**1**) determined crystallographically and shown in perspective, together with the numbering scheme adopted, in Figure 1. Although the precision of the crystallographic study is not as high as can often be achieved (data were measured at room temperature, $\theta_{max.}$ is only moderate) there is no doubt that the structure determined is correct. In particular, although the positions of the cyclohexyl carbon atoms are relatively imprecise (as evidenced by some of the carbon U_{ij} values) the central $\{P_2Au_2B_8\}$ core of the molecule is reasonably well defined.

Internuclear distances and key bond angles are given in Table 2. Compound (**1**) has crystallographically imposed C_2 molecular symmetry (primed atoms generated by the C_2 operation) and its $\{Au_2B_8H_{10}\}$ core has effective C_{2v} symmetry. Thus, although Au(6) bonds symmetrically to B(5) and B(7), 2.442(13) and 2.443(12) Å, P lies substantially (0.356 Å) off the effective mirror plane through Au(6), Au(6'), B(2), and B(2') subtending angles P–Au(6)–B(5) 129.8(3) and P–Au(6)–B(7) 147.4(3)°. Presumably the asymmetric disposition of P with respect to the gold–boron cluster, which might be responsible for the broadening of the highest-frequency ^{11}B resonance (see above), is a consequence of intramolecular crowding between the tricyclohexylphosphine ligands. The Au(6)–P distance, 2.307(3) Å, is not significantly different from that observed in 5,6-μ-$[(H_{11}C_6)_3PAu]$-*nido*-$B_{10}H_{13}$[2] [2.309 1(21) Å] and in $[(H_{11}C_6)_3PAuB_{10}H_{12}]^-$[1] [2.295 2(20) Å]. The formal oxidation state of gold in these last two complexes is +1.

At a simple level, the structure of (**1**) might be considered to be derived from its precursor, *arachno*-$B_{10}H_{12}(PPh_3)_2$, by replacement of the $\{B(6,9)H(PPh_3)\}$ fragments by $\{(H_{11}C_6)_3PAu\}$ fragments. Equally, there is a superficial similarity between (**1**) and *arachno*-6,9-Et_2NCS_2-6,9-$Au_2B_8H_{10}$ (**2**),[15] one of the relatively few other gold–boron complexes to have been fully characterised. One striking difference, however, is the Au ··· Au distance, 4.227(1) Å in (**1**) and 3.581(1) Å in (**2**). The central portion of (**2**) is drawn in Figure 2(*a*), and the polyhedral numbering system used for (**1**) was specifically chosen to facilitate comparison between the two species.

Compound (**2**) is a true *arachno* 10-vertex diauraborane,* derived from *arachno*-$[B_{10}H_{14}]^{2-}$ (**3**)[16] (Figure 2(*b*)] by subrogation of the $\{B(6,9)H_2\}^+$ units by $\{Au^{III}(Et_2NCS_2)\}^{2+}$ fragments. The formal unit with which the two $\{BH_2\}^+$ or two

* Compound (**2**) conforms to the polyhedral skeletal electron pair (PSEP) theory if (occupied) gold atomic orbitals (perpendicular to the local square plane) are involved in tangential cluster bonding. We do not agree with the tenet of previous authors[15] that this necessitates a formal gold(v) description.

Table 2. Bond lengths (Å) and angles (°) for $[(H_{11}C_6)_3PAu]_2B_8H_{10}$

Au(6)–P	2.307(3)	C(24)–C(25)	1.45(3)
Au(6)–B(2)	2.225(13)	C(25)–C(26)	1.54(3)
Au(6)–B(5)	2.442(13)	C(31)–C(32)	1.553(18)
Au(6)–B(7)	2.443(12)	C(31)–C(36)	1.541(18)
P–C(11)	1.854(12)	C(32)–C(33)	1.596(23)
P–C(21)	1.834(14)	C(33)–C(34)	1.56(3)
P–C(31)	1.820(12)	C(34)–C(35)	1.52(3)
C(11)–C(12)	1.501(17)	C(35)–C(36)	1.490(22)
C(11)–C(16)	1.485(18)	B(1)–B(1′)	1.689(18)
C(12)–C(13)	1.525(20)	B(1)–B(2′)	1.761(19)
C(13)–C(14)	1.452(23)	B(1)–B(7′)	1.761(18)
C(14)–C(15)	1.533(22)	B(2)–B(5)	1.820(19)
C(15)–C(16)	1.507(20)	B(2)–B(1)	1.772(19)
C(21)–C(22)	1.472(19)	B(2)–B(7)	1.829(18)
C(21)–C(26)	1.42(3)	B(5)–B(7′)	1.703(18)
C(22)–C(23)	1.536(23)	B(5)–B(1)	1.774(18)
C(23)–C(24)	1.38(3)		
P–Au(6)–B(2)	164.2(4)	P–C(31)–C(32)	109.6(8)
P–Au(6)–B(5)	129.8(3)	P–C(31)–C(36)	111.4(9)
P–Au(6)–B(7)	147.4(3)	C(32)–C(31)–C(36)	109.7(10)
Au(2)–Au(6)–B(5)	45.6(5)	C(31)–C(32)–C(33)	107.8(11)
Au(2)–Au(6)–B(7)	45.9(4)	C(32)–C(33)–C(34)	109.1(14)
Au(6)–P–C(11)	114.9(4)	C(33)–C(34)–C(35)	106.9(16)
Au(6)–P–C(21)	112.2(4)	C(34)–C(35)–C(36)	114.0(14)
Au(6)–P–C(31)	110.4(4)	C(31)–C(36)–C(35)	113.1(12)
C(11)–P–C(21)	106.4(6)	B(5)–B(1)–B(7′)	57.6(7)
C(11)–P–C(31)	105.0(5)	B(7′)–B(1)–B(2′)	62.6(7)
C(21)–P–C(31)	107.4(6)	B(2′)–B(1)–B(1′)	61.8(8)
P–C(11)–C(12)	116.0(8)	B(1′)–B(1)–B(2)	61.1(8)
P–C(11)–C(16)	114.4(9)	B(1)–B(2)–B(1′)	57.1(7)
C(12)–C(11)–C(16)	111.3(10)	B(1′)–B(2)–B(7)	58.7(7)
C(11)–C(12)–C(13)	113.2(11)	Au(6)–B(2)–B(5)	73.5(6)
C(12)–C(13)–C(14)	110.6(13)	Au(6)–B(2)–B(7)	73.4(6)
C(13)–C(14)–C(15)	114.3(14)	B(5)–B(2)–B(1)	59.2(7)
C(14)–C(15)–C(16)	108.4(12)	Au(6)–B(5)–B(2)	60.9(6)
C(11)–C(16)–C(15)	113.9(11)	Au(6)–B(5)–B(7′)	121.4(8)
P–C(21)–C(22)	118.8(10)	B(1)–B(5)–B(7′)	60.8(7)
P–C(21)–C(26)	115.7(12)	B(2)–B(5)–B(1)	59.1(7)
C(22)–C(21)–C(26)	117.8(14)	B(2)–B(1)–B(5)	61.8(7)
C(21)–C(22)–C(23)	113.2(12)	Au(6)–B(7)–B(2)	60.8(5)
C(22)–C(23)–C(24)	115.9(16)	Au(6)–B(7)–B(5′)	120.9(8)
C(23)–C(24)–C(25)	118.5(20)	B(2)–B(7)–B(1′)	58.7(7)
C(24)–C(25)–C(26)	111.5(18)	B(1′)–B(7)–B(5′)	61.6(7)
C(21)–C(26)–C(25)	117.7(17)		

$\{Au(Et_2NCS_2)\}^{2+}$ fragments interact, affording (**3**) and (**2**) respectively, is C_{2v}-$\{B_8H_{10}\}^{4-}$.

We believe, however, that compound (**1**) does not stand detailed structural and electronic comparison with either $[B_{10}H_{14}]^{2-}$ or $\{(Et_2NCS_2)Au\}_2B_8H_{10}$; rather that it is best compared to B_8H_{12} (**4**)[17] [Figure 2(*c*) and 2(*d*)]. Although the structure of (**4**) was determined many years ago from photographic data, and ultimately proved to be anomalous in electron-counting terms,[18] it appears, at least to us, to be correct. The $\{B_8H_8\}$ core has an open, double-envelope, six-atom face that supports two symmetric hydrogen bridges [H(s)] and two asymmetric hydrogen bridges [H(a), B(2)–H(a) 1.284 Å, B(7)–H(a) 1.470 Å (average values quoted)]. Figure 2(*d*) clearly shows that the asymmetrically bridging hydrogen atoms could, to a first approximation, adequately be described as pseudo-*endo* on B(2), B(2′). To an extent this view is supported by the observation that the (formally bridged) B(2)–B(7) connectivity, average length 1.798 Å, is insignificantly different from the (formally unbridged) B(2)–B(5) connectivity, 1.790 Å. Accepting the premise that H(a) in B_8H_{12} is *endo*-terminal, compounds (**1**) and (**4**) are clearly related, and may be conveniently partitioned into a common C_{2v}-$\{B_8H_{10}\}^{2-}$ fragment

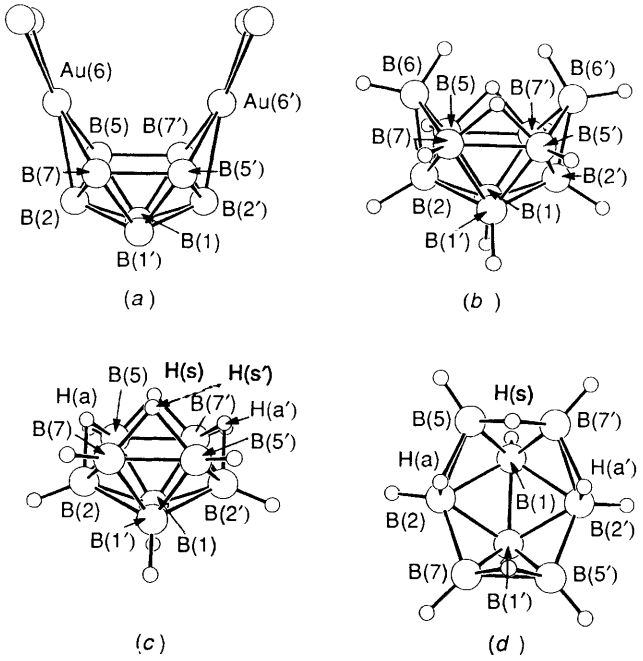

Figure 2. (*a*) Central part of $\{(Et_2NCS_2)Au\}_2B_8H_{10}$ (**2**). (*b*) $[B_{10}H_{14}]^{2-}$ (**3**). (*c*) Perspective view of B_8H_{12} (**4**). (*d*) Projection of (**4**)

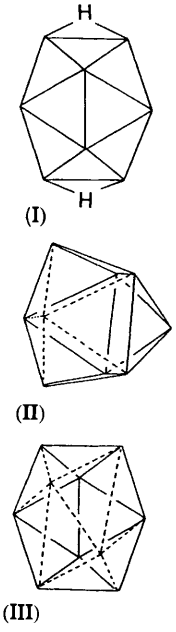

interacting, respectively, with two protons or two (isolobal) $\{(H_{11}C_6)_3PAu\}^+$ fragments.

Fragmenting species (**1**)—(**4**) as above leads to an interesting conclusion. Although a structurally similar $\{B_8H_{10}\}$ fragment (**I**) is afforded in all cases, it appears to be *formally* present in (**2**) and (**3**) as $\{B_8H_{10}\}^{4-}$, whereas in (**1**) and (**4**) the more appropriate description is as $\{B_8H_{10}\}^{2-}$. In all cases the fragments to which these units bind $[\{AuP(C_6H_{11})_3\}^+$, $\{Au(Et_2NCS_2)\}^{2+}$, $\{BH_2\}^+$, and H^+, giving (**1**), (**2**), (**3**), and (**4**) respectively] are nominally zero electron sources. In terms of the PSEP approach $\{BH_2\}^+$ and $\{Au(Et_2NCS_2)\}^{2+}$ are, in the sense of the footnote (*), two-electron sources for cluster bonding.

In a parallel project[1,19] we are currently assessing the

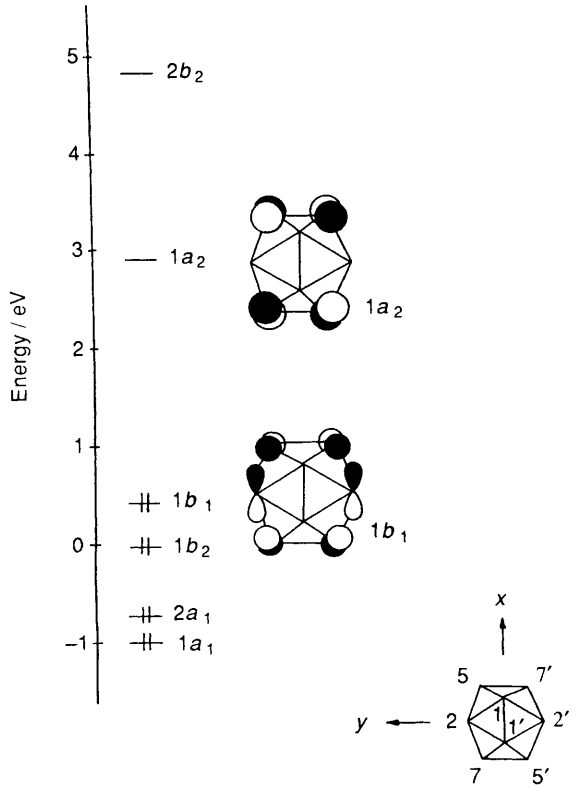

Figure 3. Frontier orbitals of the $\{B_8H_{10}\}^{2-}$ fragment, as given by EHMO calculation

possibility of distinguishing between (structurally similar) $\{B_{10}H_{12}\}^{2-}$ and $\{B_{10}H_{12}\}^{4-}$ fragments of metallaboranes, and for this purpose we make use of 'r.m.s. misfit' calculations; the lower the misfit between the common fragments of two molecules the more precise is their true structural relationship. Root mean square (r.m.s.) misfit values (Å) have been calculated from the crystallographically determined co-ordinates of the common eight boron atoms of (**1**)—(**4**) and are as follows: (**1**)—(**2**), 0.068; (**1**)—(**3**), 0.110; (**1**)—(**4**), 0.039; (**2**)—(**3**), 0.064; (**2**)—(**4**), 0.077; and (**3**)—(**4**), 0.099. Clearly, compound (**1**) fits best with (**4**), and (**2**) with (**3**), supporting the view that the structural differences between the $\{B_8H_{10}\}^{2-}$ and $\{B_8H_{10}\}^{4-}$ formalisms might be measurable. The misfit approach gives the overall fit of two fragments, and, although we believe this to be the most meaningful comparison, we have also scrutinised individual B–B distances in (**1**)—(**4**). The most marked difference lies in the (symmetrically hydrogen-bridged) B(5)–B(7′) and B(7)–B(5′) connectivities. In (**1**) and (**4**) these are (average) 1.703 and 1.687 Å respectively. In (**2**) and (**3**) they are much longer, averaging 1.786 and 1.888 Å respectively.

The compound B_8H_{12} has long been recognised as one of the very few boron hydrides that does not obey the PSEP theory first described by Wade.[18] In brief, B_8H_{12} has 10 skeletal electron pairs. It should, therefore, have the structure (**II**) of a *nido* fragment of a tricapped trigonal prism. It shows instead the structure (**III**) of an *arachno* fragment of a bicapped square antiprism. Such a skeleton would be predicted for $[B_8H_8]^{6-}$, $[B_8H_{10}]^{4-}$, and $[B_8H_{12}]^{2-}$, the last being conveniently fragmented into '$\{B_8H_{10}\}^{4-} + 2H^+$.' As far as we are aware, the fact that shape (**III**) is actually observed for '$\{B_8H_{10}\}^{2-} + 2H^+$' has never been explained.

A skeletal framework exactly analogous to (**III**) is afforded by the removal of two adjacent triangles from an icosahedron. This form, then, is predicted for the hypothetical ions $[B_8H_8]^{10-}$ and $[B_8H_{10}]^{8-}$. It is, moreover, the shape of a $\{B_8H_{10}\}^{4-}$ fragment obtained (conceptually) from $[B_{10}H_{14}]^{2-}$ by removal of the $\{B(6,9)H_2\}$ units because each of these is, in PSEP terms, a two-electron source.

In summary we can represent the essential difference between the structures of (**1**) and (**4**) (as a pair) and those of (**2**) and (**3**) (as a pair) as follows: (*i*) 2 $\{Au(Et_2NCS_2)\}^{2+}$ or 2 $\{BH_2\}^+$ units stabilise $\{B_8H_{10}\}^{4-}$ to afford 10-vertex (*arachno*) clusters that obey the PSEP theory; (*ii*) 2 $\{AuP(C_6H_{11})_3\}^+$ or 2 H^+ units stabilise $\{B_8H_{10}\}^{2-}$ to afford eight-vertex clusters that do not {thus in (**1**) the gold atom is not regarded as a true polyhedral vertex, rather it occupies a triply bridging position over the B(5)B(2)B(7) face; this complements the μ_4 bridging gold atom in $[(H_{11}C_6)_3PAuB_{10}H_{12}]^{-1}$}.

To probe the origin of this difference we have examined the frontier molecular orbitals (m.o.s) of an idealised model of $\{B_8H_{10}\}^{2-}$, and considered the effects of bringing up $2H^+$ or $2\{BH_2\}^+$ units (or their isolobal gold equivalents). The axial system employed and the key frontier m.o.s found are drawn in Figure 3. All the m.o.s represented are localised on and are outpointing from some or all of the six boron atoms in the open face.

In $\{B_8H_{10}\}^{2-}$ the occupied frontier m.o.s are $1b_1$, $1b_2$, $2a_1$, and $1a_1$. Two protons [or two $\{(H_{11}C_6)_3PAu\}^+$ cations] situated on the horizontal (yz) mirror plane have vacant orbitals of ($a_1 + b_2$) symmetry, and so would stabilise $1b_2$, $2a_1$, and $1a_1$. The lowest unfilled m.o. of $\{B_8H_{10}\}^{2-}$, $1a_2$, is cluster antibonding, particularly along the B(5)–B(7′) and B(7)–B(5′) edges.* Were this orbital to be occupied (as it is in $\{B_8H_{10}\}^{4-}$) it could not be stabilised by two protons.

In contrast, two angular (xz plane) $\{BH_2\}^+$ units [or two $\{(Et_2NCS_2)Au\}^{2+}$ cations] similarly situated have acceptor orbitals of ($a_1 + b_2 + b_1 + a_2$) symmetry, and would efficiently stabilise the occupied $1a_2$ cluster orbital, substantially reducing its antibonding character whilst at the same time affording a strong bonding interaction between the incoming fragment and B(5) and B(7).

This analysis, therefore, goes some way towards explaining the 'anomalous' structure of B_8H_{12} [and, by analogy, the gold–borane complex (**1**)]. Note, however, that it does not explain *a priori* the shape adopted by B_8H_{12}, rather it shows that, given the structure it has, this borane is more stable as the neutral species than as the PSEP-precise dianion $[B_8H_{12}]^{2-}$, since in the latter form an m.o. would be occupied that is highly destabilising.

* The formal occupation of $1a_2$ in compounds (**2**) and (**3**) [and not in (**1**) and (**4**)] nicely explains the much longer B(5)–B(7′) and B(7)–B(5′) distances in the former pair. Moreover, the more diffuse nature of the valence orbitals of gold over those of boron means that $1a_2$ will be deoccupied more when $\{B_8H_{10}\}^{4-}$ interacts with two $\{(Et_2NCS_2)Au\}^{2+}$ fragments than with two $\{BH_2\}^+$ fragments, in keeping with the shorter (by 0.1 Å) B(5)–B(7′) and B(7)–B(5′) distances in (**2**) than in (**3**).

Acknowledgements

We thank Dr. D. Reed for n.m.r. spectra, the S.E.R.C. for a studentship (to A. J. Wynd), N.A.T.O. for a travel grant, both Johnson-Matthey and the International Gold Corporation for gold salts, and the Callery Chemical Company for a generous gift of decaborane.

References

1 Part 2, A. J. Wynd, A. J. Welch, and R. V. Parish, *J. Chem. Soc., Dalton Trans.*, 1990, 2185.
2 A. J. Wynd, A. J. McLennan, D. Reed, and A. J. Welch, *J. Chem. Soc., Dalton Trans.*, 1987, 2761.

3 A. J. Wynd and A. J. Welch, *Z. Kristallogr.*, 1988, **185**, 380.
4 M. F. Hawthorne and A. R. Pitochelli, *J. Am. Chem. Soc.*, 1958, **80**, 6685.
5 CADABS, R. O. Gould and D. E. Smith, University of Edinburgh, 1986.
6 DIFABS, N. G. Walker and D. Stuart, *Acta Crystallogr., Sect. A*, 1983, **39**, 158.
7 SHELX 86, G. M. Sheldrick, University of Göttingen, 1986.
8 SHELX 76, G. M. Sheldrick, University of Cambridge, 1976.
9 'International Tables for *X*-Ray Crystallography,' Kynoch Press, Birmingham, 1974, vol. 4, p. 99.
10 CALC, R. O. Gould and P. Taylor, University of Edinburgh, 1988.
11 P. D. Mallinson and K. W. Muir, *J. Appl. Crystallogr.*, 1985, **18**, 51.
12 C. K. Johnson, Report ORNL-5138, Oak Ridge National Laboratory, Tennessee, 1976.
13 ICON 8, J. Howell, A. Rossi, D. Wallace, K. Haraki, and R. Hoffmann, Quantum Chemistry Program Exchange, University of Indiana, No. 344, 1977.
14 J. H. Ammeter, H-B. Burgi, J. C. Thibeault, and R. Hoffmann, *J. Am. Chem. Soc.*, 1982, **100**, 3686.
15 M. A. Beckett, J. E. Crook, N. N. Greenwood, and J. D. Kennedy, *J. Chem. Soc., Dalton Trans.*, 1984, 1427.
16 D. S. Kendall and W. N. Lipscomb, *Inorg. Chem.*, 1973, **12**, 546.
17 R. E. Enrione, F. P. de Boer, and W. N. Lipscomb, *Inorg. Chem.*, 1964, **3**, 1659.
18 K. Wade, *Chem. Commun.*, 1971, 792.
19 S. A. Macgregor, L. J. Yellowlees, and A. J. Welch, *Acta Crystallogr., Sect. C*, 1990, **46**, 551; *ibid.*, in the press; A. J. Wynd, S. A. Macgregor, L. J. Yellowlees, R. O. Gould, and A. J. Welch, in preparation.

Received 16*th February* 1990; *Paper* 0/00741B